Simultaneous measurement of dielectric constant and refractive index of SF 6 and CO 2 as a function of pressure

C. Adjouri, N. Balu, J. Obriot, and T. K. Bose

Simultaneous measurement of dielectric constant and refractive index of SF_6 and CO_2 as a function of pressure

C. Adjouri, N. Balu, and J. Obriot
Laboratoire POMA, Faculté des Sciences, Université d'Angers, 2B^{ld} Lavoisier, 49045 Angers Cedex 01.F, France

T. K. Bose
Institut de recherche sur l'hydrogène, Département de Physique, Université du Québec à Trois-Rivières, Trois-Rivières, Québec, G9A 5H7, Canada

Static dielectric constant ϵ and refractive index n have been measured simultaneously over a large pressure range (≈ 23 MPa). The measurements are carried out at temperatures in the supercritical region both for SF_6 and CO_2. From these static measurements, we determined the coefficients γ_1, γ_2,..., related to the linear, quadratic,..., density dependence. It is shown that the meaningful physical coefficients γ_1 are related to the integrated absorption by means of the Kramers–Kronig relation. For SF_6, the results are compared with the earlier dielectric and optical results. For CO_2, the binary coefficients γ_2 are in good agreement with the static and the absorption results. Furthermore, our results together with the accurate existing integrated absorption data demonstrate the temperature dependence of the γ_2 component. © *1997 American Institute of Physics.* [S0021-9606(97)51118-4]

I. INTRODUCTION

CO_2 and SF_6 molecules have been extensively studied in their supercritical state because of their industrial applications. More often, thermodynamic studies on macroscopic properties have been performed. However, information about the microscopic properties can be gained either from the dynamic parameters [absorption coefficient $\alpha(\nu)$] or from the static parameters (refractive index n and dielectric constant ϵ). These have been the subject of many investigations, and only some milestones will be recalled here.

Dynamic parameters for CO_2 have been determined by carrying out collision induced absorption (CIA) measurement in compressed CO_2 in the microwave[1,2] and in the far infrared.[3–5] For gaseous SF_6, collision induced infrared and far infrared absorption (FIR) measurements were reported by Rosenberg and Birnbaum,[6] Birnbaum and Sutter,[7] Joselin *et al.*[8] and Chapados and Birnbaum.[9]

Concerning the study of the static parameters during the last decade, the precision of the refractive virial coefficients have been established by several authors (e.g., Achtermann *et al.*[10] (AMB), Bose *et al.*,[11] Burns *et al.*,[12] Jaeschke *et al.*[13]). In contrast to the refractive index, much less experimental and theoretical investigations have been carried out on the dielectric constant [Bose and Cole[14] (BC), Nelson and Cole,[15] Hosticka and Bose[16] (HB), Buckingham and Pople[17]]. However, complete determination of the dielectric virial coefficient is essential for the understanding of collision induced absorption of lightwaves and comparison with the integrated absorption intensities via the Kramers–Kronig relation.[18,19]

We have developed an experimental method, the first one to our knowledge, where we are able to measure simultaneously the dielectric constant ϵ and the refractive index n. Up to now, the most commonly used method for the static

experimental determination of the second virial coefficient has been the separate measurements of ϵ and n. The basic idea of the present experiments is based on the fact that simultaneous measurements of ϵ and n in the *same thermodynamic conditions* compensate systematic errors in ϵ and n at a given frequency. We intend to show that simultaneous measurements of ϵ and n are not only fast, but also accurate.

For temperatures beyond their critical temperature, it is possible to investigate a large density region ranging from gas to liquid densities without undergoing the gas–liquid transition which usually precludes refractive index measurements. Therefore, we carried out measurements near the critical temperatures of SF_6 and CO_2 and the present work accumulated data on a large range of pressure (~ 0.50– 23 MPa).

The major aims of this paper are:

(1) The analysis of the temperature dependence of the static parameter for CO_2 and comparison with literature results.
(2) The comparison of our results with previous infrared absorption measurements (when available) by using the Kramers–Kronig relation.

For that purpose, it is emphasized here that the Kramers–Kronig relation commonly used at low densities is no more valid at high densities and must be replaced by a slightly different expression as developed in the next section.

II. THEORETICAL CONSIDERATIONS

Starting from the expressions for the complex dielectric constant and the refractive index, $\epsilon(\nu) = \epsilon'(\nu) + i\epsilon''(\nu), n^*(\nu) = n(\nu) + ik''(\nu)$; the real and imaginary parts are connected through the Kramers–Kronig relation:

$$\epsilon'(\nu) = 1 + \frac{2}{\pi} \int \frac{\nu' \epsilon''(\nu')}{\nu^2 - \nu^2} \, d\nu', \tag{1}$$

where ν is the frequency in cm^{-1} units.

The refractive index is directly related to the static dielectric constant by the relation $\epsilon = n^{*2}$, thus it results that $\epsilon'' = 2nk$. From the relation between absorption coefficient $\alpha(\nu)$, and extinction coefficient $k(\nu)$

$$\alpha(\nu) = 4\pi\nu k(\nu), \tag{2}$$

finally, Eq. (1) can be rewritten as

$$\epsilon'(\nu) = 1 + \frac{1}{\pi^2} \int \frac{n(\nu')\alpha(\nu')}{\nu'^2 - \nu^2} \, d\nu'. \tag{1'}$$

Equation (1′) shows that the dielectric constant ϵ' is not directly related to the integrated intensity in contrast to many studies at low densities where $n(\nu)$ was most commonly approximated to one. This approximation is no more valid in our case where the refractive index reaches values as high as ≈ 1.2.

In connection to this, a more suitable relation may be obtained from the optical analogue of the Kramers–Kronig relation

$$n(\nu) = 1 + \frac{2}{\pi} \int \frac{\nu' k(\nu')}{\nu'^2 - \nu^2} \, d\nu'. \tag{3}$$

Substituting expression (2) into Eq. (3), one obtains

$$n(\nu) = 1 + \frac{1}{2\pi^2} \int \frac{\alpha(\nu')}{\nu'^2 - \nu^2} \, d\nu', \tag{3'}$$

where the refractive index is now directly related to the integrated intensity.

In the following, the analysis is quite comparable to that usually made for the interpretation of the experimental results. It consists in separating the ultraviolet contributions and the infrared and lower frequency contributions,[20] so that Eq. (3′) becomes at the limit of zero frequency

$$n(0) = 1 + \frac{1}{2\pi^2} \int \frac{\alpha_{UV}(\nu')}{\nu'^2} \, d\nu'$$
$$+ \frac{1}{2\pi^2} \int \frac{\alpha_{IR}(\nu')}{\nu'^2} \, d\nu' \tag{4}$$

or

$$n(0) = n_\infty \frac{1}{2\pi^2} \nu' \int \frac{\alpha_{IR}(\nu')}{\nu'^2} \, d\nu', \tag{4'}$$

where n_∞ represents the ultraviolet contribution at zero frequency. Assuming weak dispersion, n_∞ may be replaced by n as measured in the visible region. From the Maxwell relation at zero frequency $n(0) = \sqrt{\epsilon(0)}$, Eq. (4′) can be rewritten as

$$S = \sqrt{\epsilon(0)} - n = \frac{1}{2\pi^2} \int \frac{\alpha_{IR}(\nu)}{\nu^2} \, d\nu. \tag{5}$$
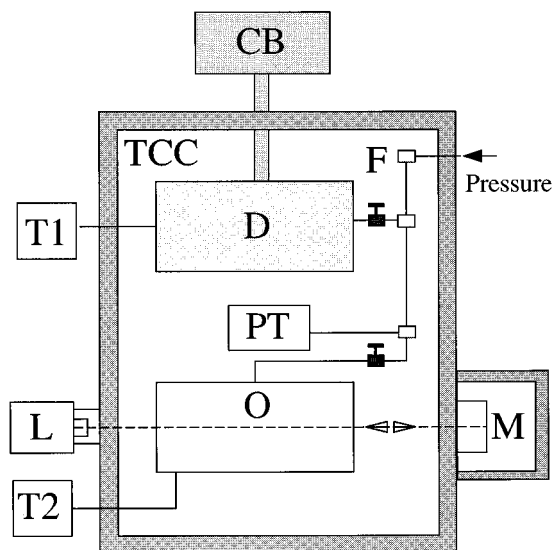

FIG. 1. Schematic diagram of the experimental setup. D: dielectric cell; CB: capacitance bridge; O: optical cell; L: laser-interferometer; M: cube corner mirror; F: filter; PT: pressure transducer; T1 and T2: calibrated thermocouples; TCC: temperature controlled chamber.

In the present work, Eq. (5) is the "backbone" relation for comparing the static and dynamic parameters. Expanding the integrated intensity in powers of the density ρ, we obtain

$$\frac{1}{2\pi^2} \int \frac{\alpha_{IR}(\nu)}{\nu^2} \, d\nu = \gamma_1 \rho + \gamma_2 \rho^2 + \gamma_3 \rho^3 + \cdots, \tag{6}$$

where $\gamma_1, \gamma_2, \gamma_3, \ldots$, account for the linear, quadratic, ternary,..., contributions. The values of γ_1 may be obtained in two ways. First, if one assumes a density expansion of the absorption coefficient in terms of $\alpha_i(\nu)$ coefficients,[3,4] we obtain for the induced binary γ_2 and ternary γ_3 coefficients

$$\gamma_i = \frac{1}{2\pi^2} \int \frac{\alpha_i(\nu)}{\nu^2} \, d\nu, \tag{7}$$

where the integration requires generally both the microwave and infrared contributions. The γ_1 coefficient is obtained in a similar way by integrating overall rotation–vibration bands in the infrared region which vary as ρ. For nonpolar molecules like CO_2, contributions arise only from vibrational transitions. Second, the γ_i coefficients can be extracted from a polynomial fit in powers of density of the simultaneous dielectric constant and refractive index values as obtained in the present experiments.

III. EXPERIMENT

Figure 1 shows a schematic of the main components of the experimental setup. This device and its application have been described elsewhere.[21,22] Briefly, the instruments consist of mainly an optical cell and a dielectric cell inside an enclosure with cooper fillings. The temperature of the cells was controlled with a circulatory waterbath and allows a temperature stability better than $\approx \pm 0.05$ K. The effective temperature was measured with thermocouples in contact

with the fluid across the cells. The pressure was measured with a quartz transducer (Paro-Scientific 740–6 K) with an uncertainty of 10^{-4}.

The dielectric measurements were made using a three-terminal parallel plate capacitance cell[22] and a decade transformer bridge (General Radio, model 1621). The precision of the capacitance measurements was 3×10^{-6} pf. A correction for the effect of pressure on the geometric capacitance of the cell was taken into account.[22]

The refractive index measurements were carried out using a standard Hewlett-Packard laser interferometer (HP-5505A) based on the heterodyne principle. The specified resolution was of the order of $\lambda/40$. The refractive index at a given pressure was obtained by counting the interference fringes when the gas under consideration reached thermodynamic equilibrium.

The optical path in the optical cell is 11.676 ± 0.05 mm. It is enclosed by two sapphire windows of 10 mm diam and 12.53 mm thick. The length of the optical cell has been optimized in order to obtain a good compromise for measurements in various pressure range: Because a small optical length produces a weak variation of the fringe count at low pressure, whereas a long optical length causes a rapid change of the fringe count namely near the critical point, where small pressure change results in large density variation.

The experimental procedure is the following. For a given monitored temperature and after temperature stabilization, the pressure is varied slowly. At each pressure and when thermodynamic equilibrium is reached, isothermal (P,n,ϵ,T) measurements are performed simultaneously. Each isotherm is covered with ≈ 80 refractive index and dielectric measurement points. Gas densities are derived with the aid of the literature virial coefficient values of HB[16] and AMB[10] for SF$_6$ and CO$_2$, respectively.

IV. DATA TREATMENT

In order to improve the accuracy of the static coefficients, we have carried out data treatment based on physical and statistical considerations and on graphical techniques. Several parameters may limit the accuracy of the coefficients in our case.

The first is the difficulty of density measurements for systems near the critical region as mentioned above: due to large density gradients, results can display dispersion. This may be the case for some of our data. In view of this and for the sake of comparison with the literature values obtained before the critical region, a simple method for the analysis of the data is described later.

The second, in the framework of classical data modeling, is the difficulty of fitting data by means of a truncated polynomial $S'[S'=f(\rho)=\Sigma_{k=0}^{n}\alpha_{k}\rho^{k}]$, a function for which the correct dependence should be a polynomial of infinite degree. In general, the truncated polynomial procedure will yield coefficients which are dependent on the degree of the polynomial fit, *especially when the data are not clustered about the intercept point of the curve on the ordinal axis*. For

example, the second order coefficient α_2 obtained from the fit of S with a cubic polynomial function may be roughly reduced by 20% when a quadratic polynomial function is used. To yield to the desired independence of coefficients, data can be fit to a function expressed as the sum of *orthogonal* polynomials (Chebyshev polynomials, polynomials involving average value, average slope, average curvature,...). The *orthogonal* polynomial coefficients α_k' are obtained as exact solution of the simultaneous least-squares equations in the orthogonal basis set. However, when switching from the orthogonal basis set to the basis related to the physical quantities, the resulting meaningful coefficients α_k'' became again dependent on the degree of the polynomial fit. Even if this procedure fails to solve the problem, it is worthwhile as a test when comparing the α_k with the α_k'' coefficients.

Finally, in an attempt to test the accuracy of different numerical methods, we perform a comparative study of data fitting with linear and nonlinear models. To summarize, the different methods used (Gauss–Newton method, Steepest descent method, Levenberg–Marquardt method, Simplex method,...) give similar results for our data within the experimental error.

In short, our γ_1, γ_2,..., coefficients determined from least-square procedure are also altered by the shortcomings described above. In order to reduce them, we perform:

(1) accurate determination of the intercept point for the data fitting,
(2) consistency test,
(3) test of the *goodness of the fit*.

For SF$_6$, the experimental values of the function $S = \sqrt{\epsilon} - n$ are combined with the value of the densities derived from HB,[16] as mentioned above. These densities are accurate within a large range and are used to perform consistency test as developed in Sec. V. In fact, below and above the critical region, the density differences between the EOS of de Reuch *et al.*[23] and those obtained from the dielectric constant measurements are of the order of 0.5% (Obriot *et al.*[21]). The SF$_6$ data reduction is implemented as follows. To ''track'' possible scattered ''outliers'' mainly in the vicinity of the critical region, we determine a first confidence region labeled C_i reasonably centered on our $S_r(\rho)=S/\rho$ values. The latter values are selected because they are more sensitive to dispersion than the $S(\rho)$ data. An estimation of the shape of the C_i region delimited by line segments is given from a first least-squares fit over all S_r values. Chi square boundary is used to limit the confidence region length. Here, the confidence interval is a region where there is an important probability for the correct parent values to fall within this region around the measured values. For each density ρ_i, the corresponding value $S_r(\rho_i)$ is compared with the lower y_l and upper y_u limits of the confidence interval. A single $S_r(\rho_i)$ value is recognized to display important dispersion if the value lies outside the interval. After recognition, we undergo a new fitting over the remaining $S_r'(\rho_i)$ values. From this new fitting, the correct final confidence interval C_f is then determined. We can be confident in the relative

merit of the data within the C_f interval which are then taken for the determination of the fitting parameters.

For densities up to 10^{-2} mol/cm^3, the best least-square fit of $S(\rho)$ for SF$_6$ was given by a polynomial of the third degree. The analysis of Achtermann *et al.*[10] based on their differential measurements demonstrate the effects related to the third refractive virial coefficients for pressures up to ≈ 7 MPa and those of higher refractive virial coefficients in the $\approx 15-35$ MPa range at 373 K. Dielectric measurements of Nelson and Cole[15] at 323 K indicate contributions of the third polarization virial coefficient at densities up to $5 \ 10^{-3}$ mol/cm^3. Our simultaneous measurements of ϵ and n at 333 K show that the contribution of the third order term is about 3% of S at 17 MPa the highest pressure investigated.

For CO$_2$, only the $S(\rho)$ data before the critical region which contribute mainly to the accuracy of the static coefficients are selected. Below the critical region, the number of scattered data are small. The static coefficients are obtained from a least-square fit of the $S(\rho)$ data. The pressure region investigated (≈ 7 to 8 MPa) is large enough, so that three-body interactions may be present. In fact, for CO$_2$, FIR absorption measurements of Birnbaum *et al.*[4] (up to 85 amagat) and those of Clouter and McKellar[5] (at ≈ 80 and 122 amagat) indicate contribution arising from ternary absorption coefficient. In our static measurements at 313 K, the contribution of the ternary term at 8 MPa is about 6% of S, and therefore, outside its experimental error.

In order to increase the accuracy of the γ, static coefficients, we measure the static parameters in the lower pressure range (≈ 0.1 to 2 MPa) in steps of 0.1 MPa and at higher pressures in steps of 0.2 MPa. Each isotherm is therefore covered with ≈ 80 static measurement points. The values of the corresponding γ_i coefficients are given in the next section.

V. RESULTS AND DISCUSSION

We carried out simultaneous measurements of the static parameters (ϵ and n) for two nonpolar molecules SF$_6$ and CO$_2$. Comparison will be made between our experimental data and absorption results based on the Kramers–Kronig relation (Sec. II) CO$_2$ is an ideal system for this kind of comparison because the collision induced spectrum is well separated from the vibrational spectrum. The case of SF$_6$ is more intricate as we shall see below.

For SF$_6$, the measurements have been carried out to relatively high pressures (≈ 17 MPa) in order to increase the contribution of the higher-order terms and hence reduce the uncertainty of the first and second static coefficients. In Fig. 2 we plotted the experimental values of the key quantity $S = \sqrt{\epsilon} - n$ for SF$_6$ for densities up to 10^{-2} mol/cm^3, and at 329.15, 333.15, and 348 K. Methods based on least-square fit of the data S to an expansion of ρ were performed as detailed in Sec. IV. In the graph S versus ρ, the γ_1 term determines the slope, the γ_2 and γ_3 terms cause the curvature of S. Our values for γ_1 and γ_2 for SF$_6$ are summarized in Table I. In the density range investigated, our data may be insufficient to obtain reliable contribution of the third static coefficient
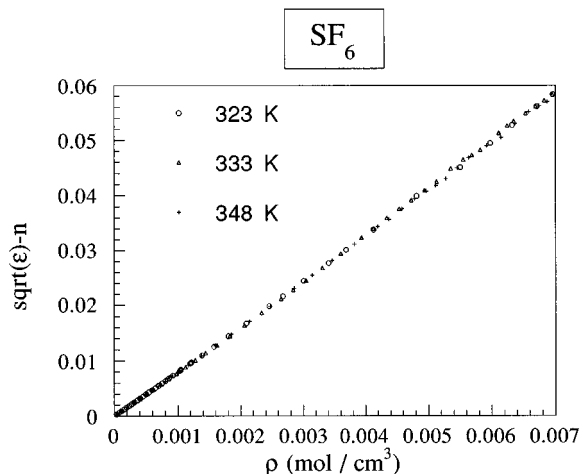

FIG. 2. Plots of the experimental static parameter $S = \sqrt{\epsilon} - n$ against the density ρ at three different temperatures for SF$_6$: (○) 323 K; (△) 333 K, and (+) 348 K.

γ_3. Assuming density development derived from the dielectric constant or refractive index values,[21] we have tested the consistency of our γ_1 and γ_2 coefficients by comparing with the values extracted from the dielectric measurements of Hosticka and Bose[16] (HB) and optical measurement of Achtermann *et al.*[10] These values are listed in the right column of Table I. The quoted uncertainties for γ_1 and γ_2 are estimated by taking standard deviations from the least-squares fit. Good agreement is found within the experimental error.

Comparative studies of the second dielectric virial coefficient and the second refractive virial coefficient of SF$_6$ suggest that there may be as yet undetected collision induced bands in the far infrared and infrared regions.[24] The search for unmeasured CIA bands motivated several infrared absorption spectroscopic experiments [Chapados and Birnbaum[9] (CB), Thomas and Linevsky[25] (TL), Delay and Thomas[26] (DT)]. CB obtained absorption spectra of gaseous and liquid SF$_6$ at temperatures from 228 to 284 K. The spectra cover the frequency range 32–3000 cm^{-1} and are recorded with a resolution of 3 cm^{-1} in the FIR, and a resolution between 1 and 2 cm^{-1} in the middle infrared (MIR) depending on the sample and the region covered. The spectra

TABLE I. The experimental values of the simultaneous static coefficients γ_1 and γ_2 for SF$_6$. The present results are compared with those deduced from the static results of Achtermann *et al.* (Ref. 10) and Hosticka and Bose (Ref. 16).

Temp. T (K)	This work		Achtermann *et al.* (Ref. 10) Hostika and Bose (Ref. 16)	
	γ_1 (cm^3/mol)	γ_2 (cm^6/mol^2)	γ_1 (cm^3/mol)	γ_2 (cm^6/mol^2)
323	7.79±0.04	109.4±5	7.83[a]	115.4[a]
333	7.73±0.05	108.5±4		
348	7.80±0.04	105.6±10	7.80[a]	111.1
373			7.88[a]	109.2

[a]Estimated, based on the temperature independence of B_R values within the small range of temperature.

are graphically displayed as $\alpha(\nu)/\rho$ versus ν, where $\alpha(\nu)$ is the absorption coefficient, ν is the frequency and ρ is the density. From their spectral analysis in the $100-3000\ \mathrm{cm}^{-1}$ range, no contribution from collision-induced component was identified in the gas phase within the experimental error.

Considering SF$_6$ as a vibrating dipole, the associated CIA contributions will be present in the same spectral range as the active vibrational lines. This will not be easy to measure in the presence of strong allowed bands, because of the generally great differences of intensity. The contributions of the CIA bands to the second dielectric virial coefficient has been estimated theoretically by Birnbaum and Bose.[24]

Thomas and Linevsky[25] (TL) made transmission measurements for SF$_6$ and derived integrated intensities of vibrational bands as a function of density and temperature. TL[25] shows a spectrum in form of absorption coefficient that covers the frequency range $1870-3500\ \mathrm{cm}^{-1}$ at 0.103, 0.689, and 2.13 MPa. Later, CIA contributions have been measured within the infrared active three-quanta vibrational bands by Delay and Thomas[26] (DT).

Although SF$_6$ is still not fully understood for the binary integrated absorption coefficient related to γ_2, comparison of the linear integrated coefficient related to γ_1 can be achieved with the aid of the compiled integrated intensities.[25,26] We have made an estimation of the linear coefficient by adding the integrated absorption of all the bands compiled by CB[9] in the $32-3000\ \mathrm{cm}^{-1}$ range and by TL[25] in the $3000-3500\ \mathrm{cm}^{-1}$ range, except for the bands attributed to collision-induced absorption. Since the main contribution to the γ_1 coefficient arise from the fundamental $\nu_4(\approx 614\ \mathrm{cm}^{-1})$ and $\nu_3(\approx 948\ \mathrm{cm}^{-1})$ bands, accurate corresponding integrated intensities A_3 and A_4 are needed. We obtain $\gamma_1 \approx 7.1\ \mathrm{cm}^3/\mathrm{mol}$ when adding all the integrated absorption together with the A_3 and A_4 values of CB,[9] and a value of $\gamma_1 \approx 7.4\ \mathrm{cm}^3/\mathrm{mol}$ when using A_3' and A_4' values averaged over different literature values.[9,27-31] These are in good agreement with our value of γ_1.

From a comparison of dielectric and pressure virial coefficients, the temperature dependence due to induced moments was studied by Hosticka and Bose[16] (HB), theoretical hexadecapole moments were derived and their sensitivity to the choice of the molecular parameters with regard to temperature dependence discussed. On the other hand, no temperature dependence was stated by TL[25] in the 296–470 K range over the restricted $1870-3500\ \mathrm{cm}^{-1}$ frequency region. However, these cannot be used directly in our case for the following reasons. First, in the spectral region investigated by TL,[25] the contribution of the integrated intensities related to γ_1 is very small, therefore no conclusion for temperature evolution of γ_1 can be given. Second, CIA contributions in the $2710-2930\ \mathrm{cm}^{-1}$ region were observed at a single temperature,[8] therefore it would not be possible to conclude on the temperature behavior of γ_2 from these results.

Concerning our results, as shown in Table I, the variation of our static coefficients in the 323–348 K temperature range are within the experimental error. This precludes any conclusion either on the temperature dependence as stated by HB[16] or on the temperature independence as follows from
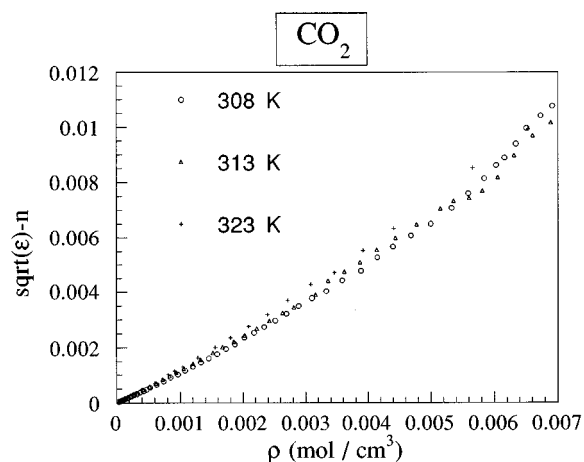

FIG. 3. Plots of the experimental static parameter S against ρ for CO$_2$ at: ($\bigcirc$) 308 K, ($\triangle$) 313 K, and ($+$) 323 K.

the Kirkwood theory.[32] Simultaneous measurements in a larger temperature range would perhaps bring more meaningful conclusions for the hexadecapole SF$_6$ system.

In Fig. 3, we plotted our experimental S values for CO$_2$ as a function of density at different temperatures. The γ_i static coefficients obtained from the least-squares fit of $S(\rho)$ (Sec. IV) are listed in Table II. The accuracy of the γ_3 coefficients may be inadequate to derive significant contribution of the third order interactions. Nevertheless, our γ_3 value of $\approx -3976.8 \pm 645\ \mathrm{mol}^3/\mathrm{cm}^9$ at 308 K may be compared with the experimental room temperature value of $\approx -5477.7 \pm 279\ \mathrm{mol}^3/\mathrm{cm}^9$ (BHR[4]) and the one of $\approx -5737.3 \pm 573\ \mathrm{mol}^3/\mathrm{cm}^9$ (DRU[33]). Up to now, only a single temperature value of γ_3 is available experimentally and the temperature dependence of this term has not been analyzed yet. BHR[4] has noted that the contribution arising from the interference effects to this ternary coefficient is negative. To the best of our knowledge, theoretical values of the ternary coefficient are not available for CO$_2$.

In contrast to this, more experimental and theoretical investigations have been made for the γ_2 coefficient related to the density square dependence of the absorption. The γ_2 coefficients determined in this work are listed together with the literature results obtained from static measurements or from microwave (2.3 cm^{-1}) and FIR absorption measurements (7–250 cm^{-1}). This kind of comparison is the first one to our knowledge. Table III shows that the compared data sets are in mutual agreement in the temperature and spectral range investigated. Although within the experimen-

TABLE II. The experimental values of the simultaneous static coefficients γ_1 and γ_2 for CO$_2$.

Temp. T (K)	γ_1 (cm^3/mol)	γ_2 (cm^6/mol^2)
308	1.04 ± 0.06	79.3 ± 8
313	1.07 ± 0.04	76.4 ± 14
323	1.13 ± 0.04	71.1 ± 7

TABLE III. Comparison of the present experimental values for γ_1 with those extracted from static and dynamic literature results for CO_2.

Temp. T (K)	This work	Dagg *et al.* (Ref. 33) $\approx \pm 10\%$	Ho *et al.* (Ref. 3) $\approx \pm 10\%$	Achtermann *et al.* (Ref. 10) Bose and Cole (Ref. 14)
296		87.7	92.9	
302				87.3[b]
308	79.3±8	77.6[a]	84.2[a]	84.4[a]
313	76.4±14	74.5[a]	81.3[a]	
323	71.1±7	68.9[a]	75.9[a]	76.9
333		63.8	70.3	

[a]Extrapolated values.
[b]Estimated based on the temperature independence of B_R values within the small range of temperature.

tal errors, differences between the γ_2 values of HBR[3] and DRU[33] are observed, this may be due to the fact that HBR[3] estimate an average value of previous microwave results for the low frequency contribution of the γ_2 integral, whereas DRU[33] take for the microwave results one deduced from their measurements at 2.3 cm^{-1}. In general, Table III shows that the static coefficients are slightly higher than the spectroscopy DRU[33] results. If information about the CIA spectrum is missing in regions where significant contribution occurs, direct application of Eq. (7) can result in an underestimation of γ_2 at most frequencies.

For CO_2, absorption coefficients in the range 1870–5000 cm^{-1} have been measured at 294, 329, and 367 K by TL.[25] The contribution of the CIA bands $2\nu_1$ and $\nu_2 + \nu_3$ occurring between ≈ 2325 cm^{-1} and ≈ 3703 cm^{-1} bands is about

$$\frac{1}{2\pi^2} \int \frac{\alpha_2(v)}{v^2} \, dv \approx 9.7 \times 10^{-4} \text{ amagat}^{-2}$$

(TL[25]) and therefore negligible and not taken into account in the present work. As far as we know, no other significant measured CIA contribution in other spectral region has been reported for gaseous CO_2.

In the following, the results of a literature search for extracting more qualitative information directly comparable to ours are presented. The data are analyzed by means of the Kramers–Kronig integral. For the sake of comparison, we have analyzed the FIR collision induced spectrum measured by Clouter and McKellar[5] (CM) at densities below the critical region. The results of CM[5] at 306 K are graphically displayed as $[\alpha(v)]/\rho^2$ versus the frequency v at two densities $\rho_1 = 80$ amagat and $\rho_2 = 122$ amagat. This may be compared with our estimate $\approx 4.5 \ 10^{-3}$ cm^{-2} amagat^2 from the BHR[4] curve at a density of 85 amagat at 295 K, although CM[5] have not integrated their values to show this. The compared values are in good agreement although the temperature of the two data sets are different and the microwave values are extrapolated from the FIR curves. Assuming a virial expansion of the form

$$\frac{\alpha(v)}{\rho^2} = \alpha_2 + \alpha_3 \rho + \cdots, \qquad (8)$$

Mannik and Stryland[34] (MK) inferred that the difference between the two absorption spectra at ρ_1 and ρ_2 indicated the effects of negative ternary contributions and possible higher order one. The negative sign and magnitude of the ternary coefficient has been discussed previously (Birnbaum *et al.*[4,35], MK,[34] DRU[33]). Assuming that the higher order collision effects are negligible, the integral related to the ternary coefficient may be deduced from the integrated expression of Eq (8) by

$$\int \frac{\alpha_3(v)}{v^2} \, dv = \frac{A_1 - A_2}{\rho_1 - \rho_2}, \qquad (9)$$

where $A_i = \int \{[1\alpha(v)]/(\rho_i^2 v^2)_i\} dv$ is the integrated absorption at the density ρ_i.

At 306 K, the absorption data of CM[5] are fairly complete in the FIR region (15–200 cm^{-1}), but no CM[5] data are available in the microwave region. Therefore, it is desirable to have some knowledge of the absorbence at one or more microwave frequencies to serve as constraints on the integration process described by A_i. Microwave values may be obtained by (i) extrapolation of the FIR results of CM[5] to low frequencies, (ii) taking advantage of the values extracted from the microwave data of DRU.[33] For example, in case (i) we obtain at 2.3 cm^{-1} $[1\alpha(v)]/(\rho_1^2 v^2) \approx 5.7 \ 10^{-8}$ amagat^{-2} for $\rho_1 = 80$ amagat, in case (ii) we have $[1\alpha(v)]/(\rho_1^2 v^2) \approx 5.9 \ 10^{-8}$ amagat^{-2} for the same conditions. At this level, the agreement (within $\approx 3\%$) between the (i) and (ii) values appear to validate the extrapolation to microwave frequency. From the $\int \{[\alpha_3(v)]/v^2\} dv$ value, together with the integrated expression of Eq. (8) for a given density, one may deduce the Kramers–Kronig integral $[1/(2\pi^2)]\int \{[\alpha_2(v)]/v^2\} dv = \gamma_2$ itself. Our estimates from the spectra of CM[5] at 80 amagat using (i) gives $\gamma_2 \approx 76.5$ cm^6/mol^2 and with (ii) a value of $\gamma_2' \approx 77.5$ cm^6/mol^2. Same value is obtained for γ_2' at 122 amagat, as a test of the density independence of γ_2'. Caution must be used, however, with regard to the value of the γ_2' coefficient, because of possible inaccuracy of this kind of indirect method. We believe, nevertheless, that this value represents a reasonable approximation to the CM[5] data. Furthermore, our estimates of $\gamma_2' \approx 77.5$ cm^6/mol^2 from the FIR spectra of CM[5] at 306 K compares favorably with our static result $\approx 79.3 \pm 7$ cm^6/mol^2 at 308 K and with the value of ≈ 77.6 cm^6/mol^2 (DRU[33]) extrapolated to the same temperature.

For the sake of comparison, Fig. 4 displays the temperature dependence T of the γ_2 coefficient and they compare reasonably well with the previous results in the 233–333 K range. Also shown in the figure are the best least-squares fit over the corresponding data. Although our data cover a small temperature range, they indicate that the γ_2 coefficient may be approximated by a $T^{-2.3}$ dependence in good agreement with the dynamic results of DRU[33] $T^{-2.5\pm0.3}$, and those estimated from HBR[3] T^{-22}. The estimates from the static results $T^{-1.9}$ (AMB,[10] BC[14]) gives a lower dependence. Detailed analysis of the interactions arising from the large quadrupole moment of CO_2 has been performed by Bose and
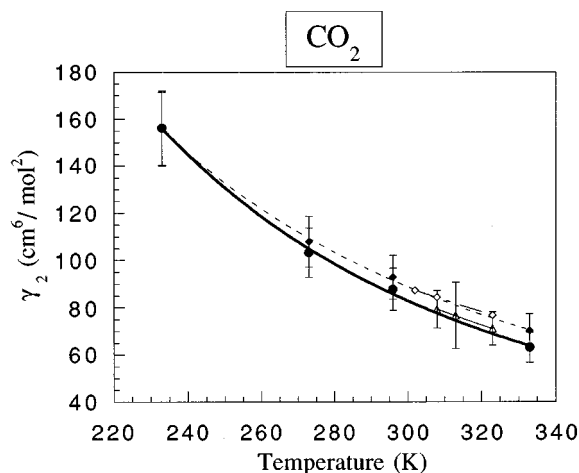
FIG. 4. Experimental comparison of the temperature dependence of γ_2 for CO_2, ($\blacklozenge$) Collision induced absorption (CIA) results of HBR (Ref. 3); ($\bullet$) dynamic values of DRU (Ref. 33); ($\diamond$) static values (Ref. 10 and 14); ($\triangle$) present simultaneous static results.

Cole[14] (BC). The corrections to the second dielectric virial coefficient have been studied accurately for the first time by BC[14] and later discussed by HBR[3] and DRU.[33]

VI. CONCLUSION

In this paper, we have emphasized the relation that exists between simultaneous dielectric and refractive index coefficients on the one hand, and the integrated absorption on the other. In this connection, we have presented for the first time a comparison between simultaneous static and dynamic measurements. The general good agreement for CO_2 indicates that the method developed in Sec. II is probably a fair representation of the actual binary absorption. In the present work, no conclusion on the temperature dependence of the static coefficients may be proposed for SF_6. In the case of CO_2, our results for the binary coefficient as well as its temperature dependence agree well with previous accurate microwave and FIR absorption results. For CO_2, precise static measurements (Hourri *et al.*)[36] may be put at the same level as collision induced absorption in the FIR, as far as binary integrated coefficients are concerned, provided that the CIA bands are exhaustively detected in the full spectral region of interest. Notice that static dielectric constants and refractive index in the limited spectral range can also be used as constraints for refractive index spectrum derived from absorption spectra in liquid and solid phase by means of Kramers–Kronig analysis (Martonchik *et al.*[37]).

ACKNOWLEDGMENTS

[1] G. Birnbaum, A. Maryott, and P. F. Wacker, J. Chem. Phys. **22**, 1782 (1954).
[2] I. R. Dagg, G. E. Reesor, and J. L. Urbaniak, Can. J. Phys. **52**, 973 (1974).
[3] W. Ho, G. Birnbaum, and A. Rosenberg, J. Chem. Phys. **55**, 1028 (1971).
[4] G. Birnbaum, W. Ho, and A. Rosenberg, J. Chem. Phys. **55**, 1039 (1971).
[5] M. J. Clouter and A. R. W. McKellar, Can. J. Phys. **63**, 1559 (1985).
[6] A. Rosenberg and G. Birnbaum, J. Chem. Phys. **52**, 683 (1970).
[7] G. Birnbaum, and H. Sutter, Mol. Phys. **42**, 21 (1981).
[8] C. G. Joslin, C. G. Gray, I. R. Dagg, A. Anderson, T. F. Gmach, and W. Smith, Can. J. Phys. **69**, 671 (1991).
[9] C. Chapados and G. Birnbaum, J. Mol. Spectrosc. **132**, 323 (1988).
[10] H. J. Achtermann, G. Magnus, and T. K. Bose, J. Chem. Phys. **94**, 5669 (1991).
[11] T. K. Bose, J. M. St-Arnaud, H. J. Achtermann, and R. Scharf, Rev. Sci. Instrum. **58**, 2279 (1986).
[12] R. C. Burns, C. Graham, and R. M. Weller, Mol. Phys. **59**, 41 (1986).
[13] M. Jaeschke, S. Audibert, P. van Caneghem, A. E. Humphreys, R. Janssen van Rosmalen, O. Pellar, J. P. J. Michels, J. A. Schouten, and C. A. Ten Sledam, VDI, Verlag Düsseldorf (1988).
[14] T. K. Bose and R. H. Cole, J. Chem. Phys. **52**, 140 (1970).
[15] R. D. Nelson and R. H. Cole, J. Chem. Phys. **54**, 4033 (1971).
[16] C. Hosticka and T. K. Bose, J. Chem. Phys. **60**, 1318 (1974).
[17] A. D. Buckingham and J. A. Pople, Trans. Faraday. Soc. **51**, 1029, 1173, 1179 (1955).
[18] T. K. Bose, *Phenomena induced by Intermolecular Interactions*, edited by G. Birnbaum (Plenum, New York, 1985), p. 49.
[19] T. K. Bose, *Collision and Interaction-Induced Spectroscopy*, edited by G. C. Tabisz and M. N. Neuman (Kluwer, Netherlands, 1995), p. 77.
[20] E. E. Bell, *Light and Matter, Encyclopedia of Physics*, edited by L. Genzel (Springer, Berlin, 1967).
[21] J. Obriot, J. Ge, T. K. Bose, and J. M. St-Arnaud, Fluid Phase Equilibria **86**, 315 (1993).
[22] J. Huot and T. K. Bose, J. Chem. Phys. **94**, 3849 (1991).
[23] K. M. de Reuch, R. J. B. Craven, and W. A. Cole, IUPAC Thermodynamic Tables Project Centre, Imperial College, London (1991).
[24] G. Birnbaum and T. K. Bose, J. Chem. Phys. **71**, 17 (1979).
[25] M. E. Thomas and M. J. Linevsky, J. Quant. Spectrosc. Radiat. Transfer **42**, 465 (1989).
[26] C. T. Delay and M. E. Thomas, J. Quant. Spectrosc. Radiat. Transfer, **48**, 3 (1992).
[27] P. N. Schatz and D. F. Hornig, J. Chem. Phys. **21**, 1516 (1953).
[28] J. H. Schachtschtscheider, Dissertation, University of Minnesota, 1960.
[29] K. C. Kim, R. C. McDowell, and W. T. King, J. Chem. Phys. **73**, 36 (1980).
[30] C. Broadbeck, I. Rossi, H. Strapelias, and J. P. Bouanich, J. Chem. Phys. **74**, 1 (1980).
[31] D. S. Dunn, K. Scanlon, and J. Overend, Spectrochim. Acta Part A **38**, 841 (1982).
[32] G. Kirkwood, J. Chem. Phys. **4**, 592 (1936).
[33] I. R. Dagg, G. E. Reesor, and J. L. Urbaniak, Can. J. Phys. **53**, 1764 (1975).
[34] L. Mannik and J. C. Stryland, Can. J. Phys. **50**, 1355 (1972).
[35] G. Birnbaum, H. B. Levine, and D. A. McQuarrie, J. Chem. Phys. **46**, 1557 (1967).
[36] A. Hourri, J. M. St. Arnaud, and T. K. Bose, J. Chem. Phys. **106**, 1780 (1997).
[37] J. V. Martonchik and G. S. Orton, Appl. Opt. **33**, 8306 (1994).